Amplification of flood frequencies with local sea level rise and emerging flood regimes

2017 Environ. Res. Lett. 12 064009

(http://iopscience.iop.org/1748-9326/12/6/064009)

Environmental Research Letters

LETTER

Amplification of flood frequencies with local sea level rise and emerging flood regimes

Maya K Buchanan[1,4], Michael Oppenheimer[1,2] and Robert E Kopp[3]

[1] Woodrow Wilson School of Public and International Affairs, Princeton University, Princeton, NJ, United States of America
[2] Department of Geosciences, Princeton University, Princeton, NJ, United States of America
[3] Department of Earth and Planetary Sciences, Rutgers Energy Institute, and Institute of Earth, Ocean, and Atmospheric Sciences, Rutgers University, New Brunswick, NJ, United States of America
[4] Author to whom any correspondence should be addressed.

E-mail: mayakb@princeton.edu

Keywords: sea level rise, coastal flooding, climate change impacts, deep uncertainty, extreme value theory, risk management

Supplementary material for this article is available online

OPEN ACCESS

RECEIVED
14 February 2017

REVISED
20 March 2017

ACCEPTED FOR PUBLICATION
12 April 2017

PUBLISHED
7 June 2017

Abstract

The amplification of flood frequencies by sea level rise (SLR) is expected to become one of the most economically damaging impacts of climate change for many coastal locations. Understanding the magnitude and pattern by which the frequency of current flood levels increase is important for developing more resilient coastal settlements, particularly since flood risk management (e.g. infrastructure, insurance, communications) is often tied to estimates of flood return periods. The Intergovernmental Panel on Climate Change's Fifth Assessment Report characterized the multiplication factor by which the frequency of flooding of a given height increases (referred to here as an amplification factor; AF). However, this characterization neither rigorously considered uncertainty in SLR nor distinguished between the amplification of different flooding levels (such as the 10% versus 0.2% annual chance floods); therefore, it may be seriously misleading. Because both historical flood frequency and projected SLR are uncertain, we combine joint probability distributions of the two to calculate AFs and their uncertainties over time. Under probabilistic relative sea level projections, while maintaining storm frequency fixed, we estimate a median 40-fold increase (ranging from 1- to 1314-fold) in the expected annual number of local 100-year floods for tide-gauge locations along the contiguous US coastline by 2050. While some places can expect disproportionate amplification of higher frequency events and thus primarily a greater number of historically precedented floods, others face amplification of lower frequency events and thus a particularly fast growing risk of historically unprecedented flooding. For example, with 50 cm of SLR, the 10%, 1%, and 0.2% annual chance floods are expected respectively to recur 108, 335, and 814 times as often in Seattle, but 148, 16, and 4 times as often in Charleston, SC.

1. Introduction

Coastal flooding is already one of the most damaging environmental hazards—responsible for a great loss of life, property, and long-term effects on municipal services and economic health (Hsiang and Jina 2014, USACE 2015). Flood height is driven by sea level rise (SLR) and storm tide, which in turn is composed of tide and storm surge. Even a small amount of SLR augments the flood height associated with a storm surge or tidal event. Indeed, flooding amplified by SLR is projected to be the most damaging market impact of climate change for many coastal regions of the US in the 21st century (Houser *et al* 2015). Understanding the magnitude and pattern by which the frequency of current flood levels (such as the 1% annual chance flood, or equivalently the 100-year flood) increase is critical for developing more resilient coastal areas, particularly since coastal infrastructure management, federal flood insurance, and flood risk

communications are typically tied to estimates of flood return periods (e.g. NYC 2013, Douglas *et al* 2016).

The amplification factor (AF) is a metric that measures the change in the expected frequency of a historic annual chance flood with SLR. It has been calculated explicitly (Hunter 2012, Church *et al* 2013) and implicitly (by estimating changes in flood frequency; Tebaldi *et al* 2012, Lin *et al* 2012) to aid stakeholder decision-making about coastal flood risk management. AFs are a function of the frequency distribution of storm tide events and the amount of local SLR—both of which are uncertain (see section 3). Storm tide distributions can be simulated with hydrodynamic models, which may then be fit by an extreme value distribution to estimate the storm tide frequency distribution (including or excluding SLR, e.g. Lin *et al* 2012 and Muis *et al* 2016, respectively). Alternatively, observations can be fit to an extreme value distribution to estimate a storm tide distribution, which can be adjusted for the distribution of future SLR. Extreme value theory is commonly used because of the computational intensity of high-resolution hydrodynamic modeling and also because it is data-based, capturing both tropical and non-tropical storm surges. Although hydrodynamic modeling can simulate potential changes in storm surges associated with tropical cyclones in response to warming sea surface temperatures and changing wind patterns, there is low confidence in climate model projections of future tropical cyclone behavior, particularly in individual basins (e.g. Knutson *et al* 2010). Here, we assume there are no significant changes in tides or storm climatology that would affect storm tide distributions.

The Gumbel extreme value distribution was prominently used in the Intergovernmental Panel on Climate Change's (IPCC) Fifth Assessment Report (AR5; Church *et al* 2013) and elsewhere (Hunter 2012, Muis *et al* 2016) because it has the advantage of simplicity, assuming an exponential relationship between the level and frequency of flooding. However, AFs estimated by it are invariant to flood levels and do not capture the distinct effects of SLR on flooding in areas with heavy- and thin-tailed flood frequency distributions. Here we present calculations of the amplification of flood return periods using extreme value theory allowing for heavy- and thin-tailed distributions and their change with SLR. We combine joint probability distributions of flood frequency using the Generalized Pareto Distribution (GPD), incorporating uncertainty in this extreme value distribution and employing probabilistic local SLR projections (conditional upon a greenhouse gas emissions pathway) to provide AFs along US coastlines for various flood levels, timeframes, and SLR scenarios.

2. Estimating the amplification of flood frequencies

There are two main families of extreme value distributions: the Generalized Extreme Value (GEV) distribution and GPD. The GEV family of distributions is used in block maxima analysis, in which extremes are estimated by maximum water levels over a unit of time (e.g. annual values). The GPD is used in peak-over-threshold (POT) analysis, in which the probability of having an event over a specified threshold is described by a Poission distribution and the GPD characterizes the conditional probability of an event of a given magnitude. In a POT analysis, all observations over a high threshold (e.g. the 99th percentile of hourly water levels; Tebaldi *et al* 2012) are used to estimate the distribution of flood events (e.g. water level extremes). Hence, the GPD incorporates sub-annual maxima, making use of more of the available data. For these reasons, the GPD has been recognized as a hydrological standard since 1975 (NERC 1975, Coles *et al* 2001).

The number of exceedances of flood level z for the GEV and Poisson–GPD are given by:

$$N(z) = \begin{cases} \lambda\left(1 + \dfrac{\xi(z-\mu)}{\sigma}\right)^{\frac{-1}{\xi}} & \text{for} \quad \xi \neq 0 \\ \lambda \ \exp\left(-\dfrac{z-\mu}{\sigma}\right) & \text{for} \quad \xi = 0 \end{cases} \tag{1}$$

whereby the distributions are characterized by location (μ), scale (σ), and shape (ξ) parameters. The location parameter relates to local sea level, the scale parameter to the variability in the maxima of water level caused by the combination of tides and storm surges, and the shape parameter to the curvature and upward limit of a flood frequency curve. These expressions for the number of exceedances in the GEV and Poisson–GPD are identical except for λ. For the Poisson–GPD, λ is the Poisson-distributed annual mean number of flood events; for a GEV describing annual block maxima, $\lambda = 1$ event/year (Hunter 2012, Buchanan *et al* 2016). For $\xi = 0$, the expression is identical to that for a Gumbel distribution, a simple exponential function (figure 1(*a*)).

The shape parameter dominates the tail of a flood frequency distribution (Coles *et al* 2001), illustrated by the distinction between curves in figure 1(*a*) from only a variation in ξ, holding all other parameters constant. Flood frequency distributions with $\xi > 0$ are 'heavy-tailed', with a relatively high frequency of extreme flood levels. Conversely, flood frequency curves with $\xi < 0$ are 'thin-tailed', having an upper bound of extreme flood levels.

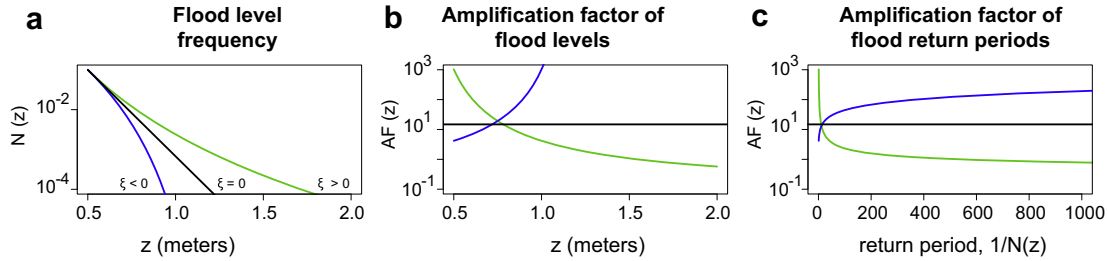

Figure 1. (*a*) Flood frequency distributions (the number of expected events of flood level *z*), (*b*) amplification factors (AFs) of flood levels *z*, and (*c*) AFs of corresponding return periods (1 / *N*(*z*)) for 0.5 m SLR and three hypothetical GPD curves with equal parameters except for varying shape factors (ξ). The green, blue and black lines correspond to a positive ($\xi = .15$), negative ($\xi = -.15$), and zero ξ. The AF of a given flood level *z* is dependent on the sign of the extreme value shape parameter.

The AF of a flood of height z after SLR is $N(z-\delta)/N(z)$, where $N(z-\delta)$ is the new expected number of exceedances of the flood level with SLR:

$$\mathrm{AF}(z) = \frac{N(z-\delta)}{N(z)} = \begin{cases} \left(1 - \dfrac{\delta}{(\sigma/\xi) + z - \mu}\right)^{\frac{-1}{\xi}} & \text{for } \xi \neq 0 \\ \exp\left(\dfrac{\delta}{\sigma}\right) & \text{for } \xi = 0 \end{cases} \quad (2)$$

Taking the derivative of AF(z) with respect to z shows the dependence of the AF on flood height:

$$\frac{\partial \mathrm{AF}(z)}{\partial z} = \begin{cases} \dfrac{-\delta\xi[\mathrm{AF}(z)]^{(1+\xi)}}{(\xi(z-\mu)+\sigma)} & \text{for } \xi \neq 0 \\ 0 & \text{for } \xi = 0 \end{cases} \quad (3)$$

Assuming AF(z) and $\delta > 0$, the sign of $\partial \mathrm{AF}(z)/\partial z$ is equal to the sign of $-\xi$, so the AF is decreasing with flood height for positive shape factors and increasing with flood height for negative shape factors (figures 1 (*b*) and (*c*)).

For $\xi = 0$ (i.e. a Gumbel distribution), $\partial \mathrm{AF}(z)/\partial z = 0$; there is no dependence of AF on flood height, and thus its use assumes AFs are invariant to flood levels; i.e. that all flood frequencies amplify by the same magnitude (figures 1(*b*) and (*c*)). A key question thus arises among the approaches in extreme value theory to fit a distribution to flood frequencies—whether to use the simple Gumbel distribution or the GPD/GEV that requires fitting of a shape parameter. Because the shape parameter is dominant in determining a flood frequency distribution, there is a trade-off between the simplicity of the extreme value distribution used and its validity (Coles *et al* 2001). Simple approximations are more tractable numerically; however, they are suboptimal when another accessible approach can differentiate between varying values of key metrics of concern—such as changes in the recurrence of the 10-year vs 500-year flood under climate change.

Amplification of flooding frequency is also heavily influenced by how local SLR is characterized. Under uncertain SLR, the AF equals $\mathbb{E}[(N(z)-\delta)/N(z)]$. By Jensen's inequality (Jensen 1906), the convex transformation of the expectation of a random variable is less than or equal to the expectation of the convex transformation of the random variable. As a result of Jensen's inequality and the approximate log-linearity of flood frequency curves, the AF under expected SLR is less than the expected AF under uncertain SLR, such that $\mathbb{E}[(N(z)-\delta)/N(z)] \geq N(z-\mathbb{E}[\delta])/N(z)$. This inequality holds even if the distribution of SLR is symmetric, and the discrepancy is larger still if the distribution is positively skewed (i.e. when expected SLR is greater than median SLR). Because $N(z)$ is also a random variable, accounting for the uncertainty in the extreme value distribution fit is also important.

3. Methods

3.1. Extreme value theory

We analyze National Oceanic and Atmospheric Administration (NOAA) hourly tide-gauge records for sites with a minimum 30 year record (which can be found at http://tidesandcurrents.noaa.gov/) following the methodology of Tebaldi *et al* (2012) and Buchanan *et al* (2016). The GPD is estimated using hourly water level exceedances above a high threshold (equal to the 99th percentile of the hourly water level; Gilleland and Katz 2011). Hourly tide records are used to capture storm surge, astronomical tides, and interannual sea level variability, and are detrended to remove the contribution of changes in mean sea level. To account for uncertainty in fit, GPD parameters are estimated by maximum likelihood, and their covariance is estimated based on the observed Fisher information matrix (the Hessian of the negative log-likelihood at the maximum-likelihood estimate). We sample 1000 parameter pairs with Latin hypercube sampling, assuming the parameter uncertainty is normally distributed. The expected number of exceedances under parameter uncertainty is calculated for our main calculations. Below the GPD threshold of λ events per year, we fit a Gumbel distribution with 182.6 events exceeding mean higher high water (MHHW) per year, assuming about half of all days have higher high water levels above mean higher high

water. For a comparative analysis, a Gumbel distribution is also fitted to the full distribution of threshold exceedances.

3.2. Sea level rise projections

We use 10 000 Monte Carlo samples of Kopp *et al* (2014) local SLR projections, accounting for global and local contributions, including land subsidence, distributional effects of land-ice melt (SLR fingerprints), and expert assessment of dynamic ice-sheet collapse. These SLR projections are asymmetric, and—due primarily to the poorly constrained but potentially large contribution of the Antarctic ice sheet (e.g. DeConto and Pollard 2016)—positively skewed. We use two Representative Concentration Pathways (RCP) 4.5 and 8.5 which represent greenhouse gas concentrations that lead to a radiative forcing of 4.5 and 8.5 W m^{-2} by 2100 (Van Vuuren *et al* 2011).

3.3. Amplification factors

The distribution of AFs and the expectation over 1000 samples of the AF are calculated for a given site. In our main calculations, AFs estimated by the GPD include uncertainty in local SLR and in the GPD fit, while AFs estimated by the Gumbel distribution include uncertainty in local SLR.

4. Amplification of current flood levels with sea level rise

The shape factors, ξ, reflect meteorological and hydrodynamic differences among sites (figure 1(*a*) in Buchanan *et al* 2016). Exposed to tropical cyclones, sites along the Gulf and Atlantic coasts tend to have heavy-tailed flood frequency distributions, with positive ξ. Conversely, sites along the Pacific coast, limited by steeper coastal slopes into the seabed and fewer barrier beaches (Pugh 1996), tend to have thin-tailed distributions, with negative ξ.

The sensitivity of flood frequency distributions to ξ (Coles *et al* 2001) yields distinct behavior: AFs increase as a function of z when $\xi > 0$, decrease as a function of z when $\xi < 0$, and are greatest for z at which the slope of $N(z)$ is steepest. Hence, sites with positive ξ face a large amplification of traditionally less extreme storm tide, whereas those with negative ξ face high amplification of traditionally extreme storm tide.

Sea level rise not only amplifies flood heights but also changes the relation of flood height to flood frequency across locations. We refer to the relationship between flood height and flood frequency changes under SLR as an emerging flood regime. It can be simply illustrated by the ratio of the AF of the 500 year flood to the AF of the 10 year flood (R_{AF}). Take, for example, the flood frequency distributions of four US tide gauge sites with varying ξ: Charleston, SC with a large positive shape factor ($\xi = 0.23$ [0.10, 0.36]; maximum-likelihood, median [5th and 95th percentiles]), New York City with a more moderately positive shape factor ($\xi = 0.19$ [0.07, 0.30]), San Francisco with a near-zero shape factor ($\xi = 0.03$ [−0.10, 0.16]), and Seattle, WA with a large negative shape factor ($\xi = -0.17$ [−0.27, −0.06]; figure 1). Fifty cm of local SLR amplifies the 10-year, 100-year, and 500-year floods by 148, 16, and 4 times in Charleston (yielding a R_{AF} of 0.03) and by 109, 335, and 814 times in Seattle ($R_{AF} = 7.47$). AFs are less divergent across $N(z)$ for places with smaller ξ (in absolute value): R_{AF} is 0.17 in New York and 0.43 in San Francisco.

The Gumbel distribution fits the majority of observations of extreme water levels poorly. For a subset of qualifying sites, we define $\triangle$AIC as the difference between the Akaike Information Criterion (AIC) with the Gumbel distribution and the AIC with the GPD, whereby lower AIC values indicate higher model quality. The $\triangle$AIC is negative for only 5 out of 23 sites and has a mean of 11.77 and *s.d.* of 6.97 (supplementary table 4 available at stacks.iop.org/ERL/12/064009/mmedia). When ξ is assumed to be zero, the AF is reduced to a single scalar, invariant to flood level—196 for Charleston and 86 for Seattle (equation (2)). This underestimates the recurrence of the 500-year flood in Seattle and overestimates it in Charleston by 1–2 orders of magnitude, respectively (figure 2, columns *G* and *GPD*). This illustrates the Gumbel distribution's poor approximation for storms far in the tail and reflects the larger problem with using the Gumbel distribution to estimate flood frequencies. Accounting for uncertainty in the GPD significantly widens the distribution of AFs for sites with positive ξ, with more uncertainty in the far tail of storm surges (columns for *Uncertain SLR* and *Uncertain GPD* in figure 2; see Methods).

AFs are also sensitive to the characterization of SLR. Using the GPD and a central estimate of SLR—rather than a probability distribution—underestimates by an order of magnitude the AF of the 500-year flood for places with negative ξ and by two orders of magnitude the AF of the 10-year flood for places with positive ξ (columns for $\mathbb{E}[SLR]$ and *Uncertain SLR* in figure 2). The expected AFs for Seattle and San Francisco are much larger than the median estimate partly because of the large positive skewness in their local SLR distributions.

Figure 3 shows the expected amplification of the current 10-year flood and its ratio to other flood levels for a set ($N = 69$) of long-duration tide gauges across US coastlines under RCP 4.5, corresponding to a likely global mean temperature increase of 2 °C–3.6 °C by 2100 (Van Vuuren *et al* 2011). While the Gumbel distribution underestimates and overestimates the AF of the current 500-year flood by 1–2 orders of magnitude (figures 3(*d*) and (*h*)), the GPD captures distinct flood regimes—the heightened AF of more extreme flooding for areas with negative ξ (and the opposite for areas with positive ξ; figures 3(*b*), (*c*), (*f*) and (*g*)). AFs in figure 3 are drastically different than those for the US in the AR5

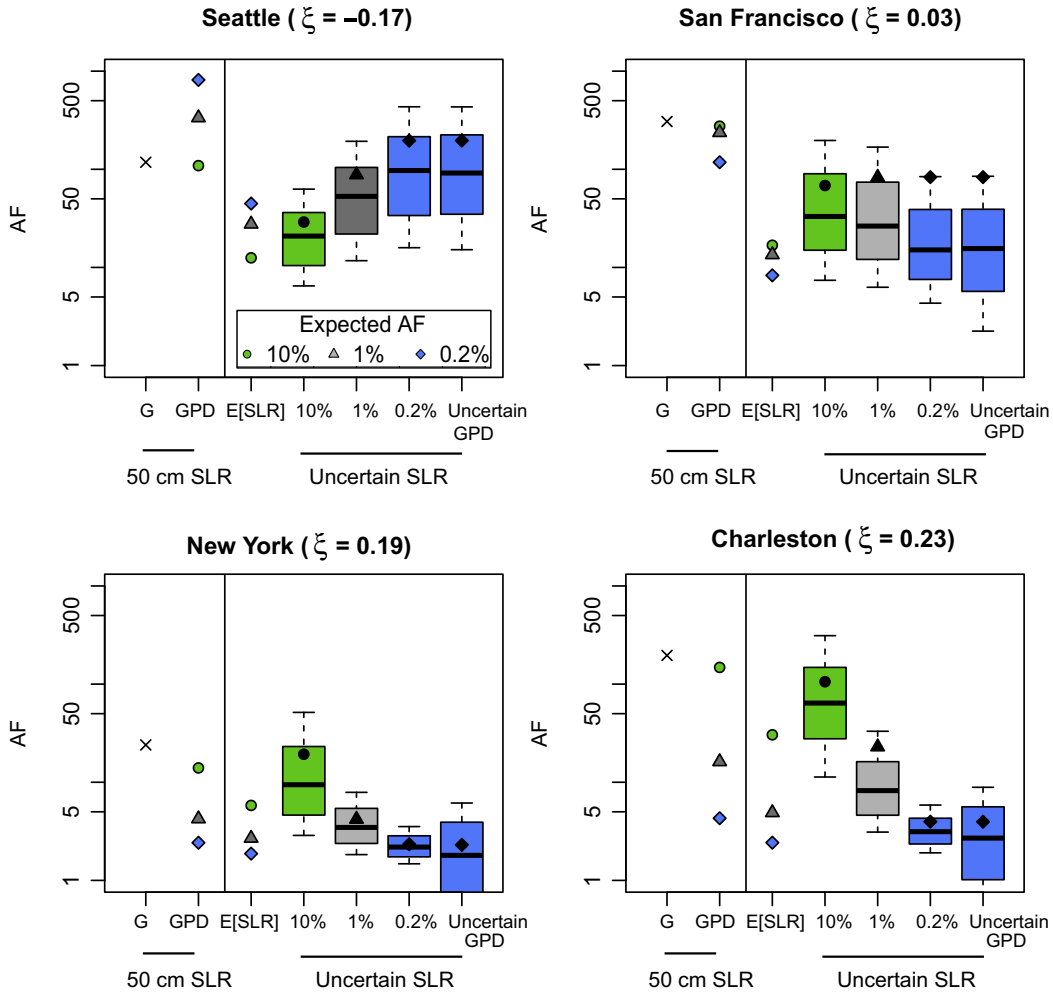

Figure 2. Expected amplification factors (AFs) of different flood return levels (10% (○), 1% (△), and 0.2% (◇) annual chance floods) for different extreme value distributions (*GPD and Gumbel*) and characterizations of sea level rise (SLR) for sites (Seattle, San Francisco, Charleston, and New York City) with varying shape parameters (negative, near-zero, and positive ξ). Amplification scenarios include: (1) the Gumbel distribution with 0.5 m deterministic SLR (column *G*), (2) the GPD with 0.5 m deterministic SLR for the 10-, 100-, and 500 years floods (*GPD*), (3) the GPD with expected SLR for 2050 under RCP 4.5 for the 10-, 100-, and 500-year floods ($\mathbb{E}[SLR]$), (4–6) the GPD with uncertain SLR for 2050, integrated over the full probability distribution for SLR under RCP 4.5 for the 10-, 100-, and 500-year floods (*Uncertain SLR*), and finally (7) the GPD with uncertain SLR for 2050, integrated over the full probability distribution for SLR under RCP 4.5 and accounting for uncertainty in the GPD fit (see Methods) for the 500-year flood (*Uncertain GPD*). With the Gumbel distribution, differences in the expected amplification of various flood levels with the same amount of SLR are undetectable (×). The extreme value distribution (*Gumbel* vs. *GPD*) and use of only the expected level of SLR are responsible for the largest degrees of error in flood frequencies with respect to SLR. Boxplots correspond to the 5th, 17th, 50th, 83rd, and 95th percentiles of the distribution of AFs. Median estimates of the shape factor are shown in the panel titles.

figure 13.25 (Church *et al* 2013), which used a Gumbel distribution. With 50 cm of SLR, the AR5 underestimates the AF of the 500-year flood in areas with a negative ξ and overestimates it in areas with positive ξ by 1–3 orders of magnitude, respectively.

Under probabilistic relative sea level projections of Kopp *et al* (2014) for RCP 4.5 and when accounting for uncertainty in the GPD, we project a median 25-fold increase (range of 1- to 914-fold) in the expected annual number of local 100-year floods for tide-gauge locations along the contiguous US coastline by 2050 (measured with respect to detrended sea level over the entire length of the record; Buchanan *et al* 2016). These values jump significantly by 2100 (median: 1729, range: 5–12 546). As SLR gets to such high levels, lower flood levels saturate first, yielding flooding influenced primarily by tidal events rather than storm surges, and dampening the growth of the AF of all flood levels along all coastlines (figures 3(*e*), (*g*) and (*h*)). This effect is also illustrated by the red curve in online supplementary figure 1, demarcating flood levels in 2100. Under RCP 8.5, a high greenhouse gas emissions pathway, a median 40-fold increase (range: 1–1314) in the annual number of local 100 year floods is expected by 2050 and a median 3467-fold increase (range: 5–16 829) by 2100. For illustrative purposes, the current 100-year flood in Seattle is expected to occur 50.9 times a year, equal to an average of one 100-year flood per week. The expected AFs of various flood levels by 2050 and 2100 under RCP 4.5 and 8.5, accounting for uncertainty in the GPD fit, are provided in online supplementary tables 1–2. Annual expected flood frequencies of the 10-year, 100-year,

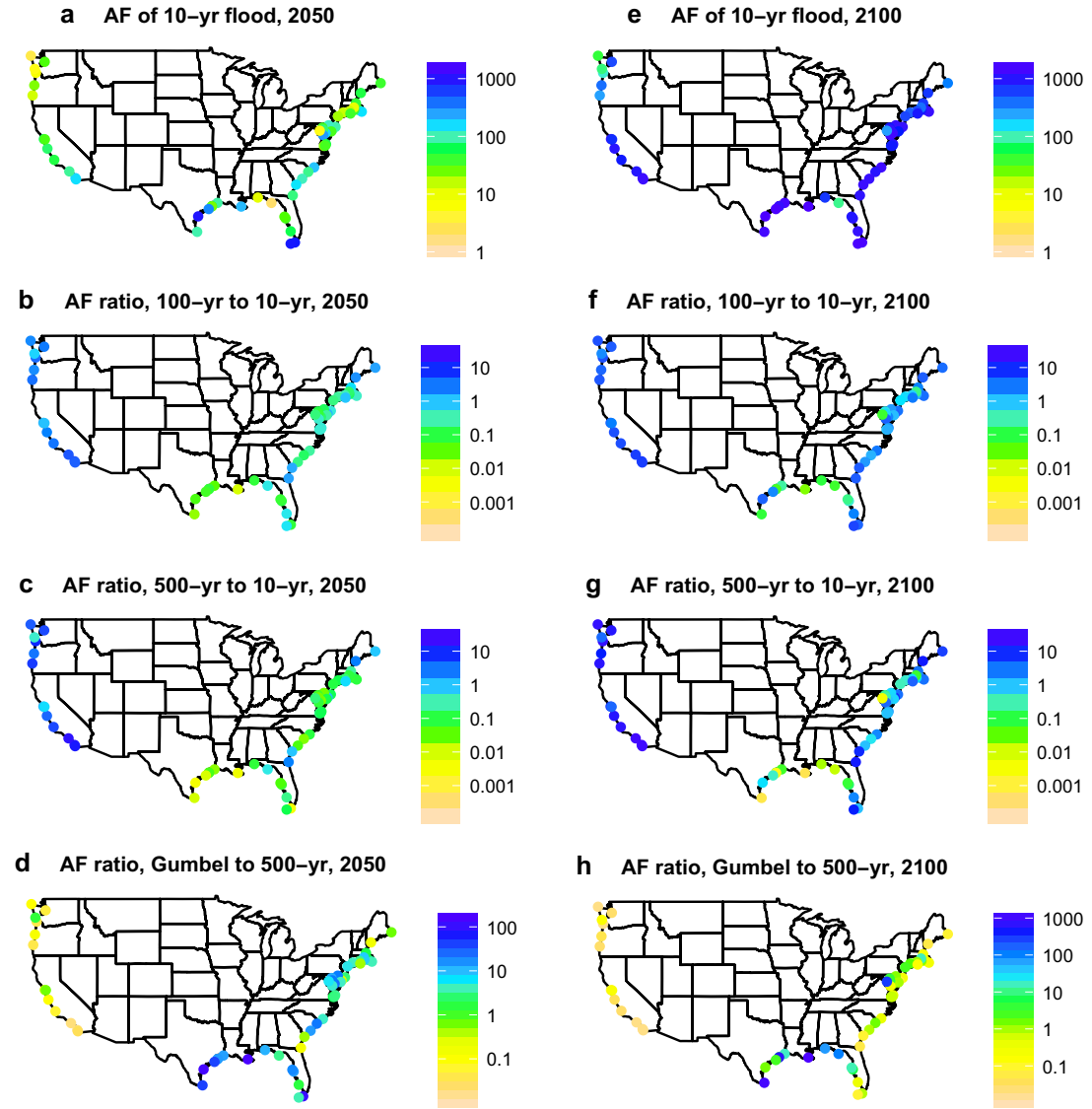

Figure 3. Amplification factors (AFs) and ratios thereof estimated for 2050 (*a*)–(*d*) and 2100 (*e*)–(*h*) under uncertain local sea level rise under RCP 4.5. (*a*), (*e*) AF of current 10 year flood return levels estimated by the GPD, (*b*), (*f*) the ratio of the AFs of the 100- to 10 year flood estimated by the GPD, (*c*), (*g*) the ratio of the AFs of the 500- to 10 year flood estimated by the GPD, and (*d*), (*h*) the ratio of the AFs estimated by the Gumbel distribution to the 500 year flood estimated by the GPD. All GPD AFs account for uncertainty in the GPD fit.

and 500-year floods by 2050 and 2100 are in online supplementary tables 5 and 6.

It should be noted that the distributions of tropical and extra-tropical cyclones may be systematically different and the significance of any such difference is unknown. Here, contributions of tropical and extra-tropical cyclones are combined as in other studies (e.g. Hunter 2012, Tebaldi *et al* 2012). Separation of these storm events would likely lead to a scarcity of very extreme events. Inclusion of uncertainty in the extreme value distribution helps account for potential sensitivity of the shape parameter to different storm events.

5. Conclusion

SLR imposes slow but steady inundation of coastal land and property. However, the more immediate threat from SLR is an amplification of flooding, independent of any potential changes in the distribution of coastal storms from climatological factors (Houser *et al* 2015, Church *et al* 2013). Amplification of current flood levels and emerging flood regimes have critical implications for cities, states, and federal entities interested in adapting to coastal impacts.

The expected amplification of flooding frequency is highly sensitive to the characterization of SLR and flood frequency curves; the commonly used Gumbel extreme value distribution can, depending on ξ, underestimate or overestimate—flood extreme increases in the far tail. Its use cannot distinguish emerging flood regimes, the pattern by which flood frequency responds to SLR. Among the prominent uses of the Gumbel distribution was the IPCC AR5 (Church *et al* 2013). Additionally, Muis *et al* (2016)

use the Gumbel distribution to derive a global data set of extreme sea levels; this data now populates the Dynamic Interactive Vulnerability Analysis (DIVA) model, which is used extensively to assess impacts of sea level rise (e.g. Hinkel *et al* 2014). The AR5 amplification values may be seriously misleading because using the Gumbel distribution implies that amplification of flood frequency is invariant across flood levels. For example, this assumes that the frequency of extreme events like a 500-year flood will increase by the same magnitude as lesser extremes, potentially projecting overly catastrophic flood hazards in some areas while underestimating flood hazards elsewhere. Prominent use of the Gumbel distribution in the IPCC—which has a special influence on policy makers—and elsewhere creates a risk that policy makers will implement policy based on the wrong information. While using a rule of thumb (implicit in the Gumbel distribution) is practical, it over-simplifies flood hazard characterization and could result in costly misjudgments by planners. This is particularly important as coastal areas tend to be early adopters of climate change adaptation planning (nearly 80% of US adaptation plans in a recent meta-analysis were in coastal states; Woodruff and Stults 2016). The use of the GPD is therefore preferable for flood risk assessment of the emerging non-stationary climate.

Using the GPD, locations with positive ξ (like New York City, Baltimore, Washington DC, and Key West) can expect disproportionate amplification of higher frequency events, whereas those with negative ξ (such as Seattle, San Diego, and Los Angeles) can expect a disproportionate amplification of lower frequency flooding. Effective policies should initially increase resilience to historical flooding in areas with emerging flood regimes associated with positive ξ, and prepare for largely unprecedented flooding in areas with negative ξ. Policies should also allow for adjustment over time to address eventual flooding dominated by tidal events and permanent inundation (Sweet and Park 2014). Identification of areas with similar flood regimes by shape factor could facilitate the sharing of adaptation strategies across coastal areas.

Acknowledgments

Support for this work was provided for M K B and M O by the National Science Foundation under Award EAR-1520683. We thank Claudia Tebaldi for her assistance in developing the extreme value distributions.

References

Buchanan M K, Kopp R E, Oppenheimer M and Tebaldi C 2016 Allowances for evolving coastal flood risk under uncertain local sea-level rise *Clim. Change* **137** 347–62

Church J A *et al* 2013 Chapter 13: sea level change *Climate Change 2013: The Physical Science Basis. Contribution of Working Group I to the Fifth Assessment Report of the Intergovernmental Panel on Climate Change* ed T F Stocker, D Qin, G K Plattner, M Tignor, S K Allen, J Boschung, A Nauels, Y Xia, V Bex and P Midgley (Cambridge University Press) pp 1137–1216 (https://doi.org/10.1017/CBO9781107415324.026)

Coles S, Bawa J, Trenner L and Dorazio P 2001 *An Introduction to Statistical Modeling of Extreme Values* (London: Springer)

DeConto R M and Pollard D 2016 Contribution of Antarctica to past and future sea-level rise *Nature* **531** 591–7

Douglas E *et al* 2016 Climate change and sea level rise projections for Boston: the Boston Research Advisory Group Report *Technical report* (Boston, MA: Climate Ready Boston)

Gilleland E and Katz R W 2011 New software to analyze how extremes change over time *Eos, Trans. Amer. Geophys. Union* **92** 13–20

Hinkel J, Lincke D, Vafeidis A T, Perrette M, Nicholls R J, Tol R S, Marzeion B, Fettweis X, Ionescu C and Levermann A 2014 Coastal flood damage and adaptation costs under 21st century sea-level rise *Proc. Natl Acad. Sci.* **111** 3292–7

Houser T, Hsiang S, Kopp R and Larsen K 2015 *Economic Risks of Climate Change: An American Prospectus* (New York: Columbia University Press)

Hsiang S M and Jina A S 2014 The causal effect of environmental catastrophe on long-run economic growth: evidence from 6700 cyclones *Technical report* (National Bureau of Economic Research)

Hunter J 2012 A simple technique for estimating an allowance for uncertain sea-level rise *Clim. Change* **113** 239–52

Jensen J L W V 1906 Sur les fonctions convexes et les inégalités entre les valeurs moyennes *Acta Math.* **30** 175–93

Knutson T R, McBride J L, Chan J, Emanuel K, Holland G, Landsea C, Held I, Kossin J P, Srivastava A and Sugi M 2010 Tropical cyclones and climate change *Nat. Geosci.* **3** 157–63

Kopp R E, Horton R M, Little C M, Mitrovica J X, Oppenheimer M, Rasmussen D, Strauss B H and Tebaldi C 2014 Probabilistic 21st and 22nd century sea-level projections at a global network of tide-gauge sites *Earth's Future* **2** 383–406

Lin N, Emanuel K, Oppenheimer M and Vanmarcke E 2012 Physically based assessment of hurricane surge threat under climate change *Nat. Clim. Change* **2** 462–7

Muis S, Verlaan M, Winsemius H C, Aerts J C and Ward P J 2016 A global reanalysis of storm surges and extreme sea levels *Nat. Commun.* **7** 11969

NERC 1975 Flood studies report *Technical report* (London: National Environment Research Council)

NYC 2013 A stronger, more resilient New York *New York City Technical Report*

Pugh D T 1996 *Tides, Surges and Mean Sea-level (Reprinted with Corrections)* (Hoboken, NJ: Wiley)

Sweet W V and Park J 2014 From the extreme to the mean: acceleration and tipping points of coastal inundation from sea level rise *Earth's Future* **2** 579–600

Tebaldi C, Strauss B H and Zervas C E 2012 Modelling sea level rise impacts on storm surges along US coasts *Environ. Res. Lett.* **7** 014032

USACE 2015 North Atlantic coast comprehensive study: Resilient adaptation to increasing risk *Technical report* (US Army Corps of Engineers)

Van Vuuren D P *et al* 2011 The representative concentration pathways: an overview *Clim. Change* **109** 5–31

Woodruff S C and Stults M 2016 Numerous strategies but limited implementation guidance in US local adaptation plans *Nat. Clim. Change* **6** 796–802